*Paper No. 1790. (quote when citing this article)*
Eleventh World Conference on Earthquake Engineering
ISBN: 0 08 042822 3

# CHARACTERISTICS OF EARTHQUAKES IN THE MEXICAN SUBDUCTION ZONE ON STRONG MOTION ACCELEROGRAMS

JOHN G. ANDERSON, ROBERTO QUAAS, QINGBIN CHEN, DAVID ALMORA, RICARDO VAZQUEZ, JUAN MANUEL VELASCO, CITLALI PEREZ, GERARDO CASTRO

Seismological Laboratory and Department of Geological Sciences,
University of Nevada, Reno, Nevada 89557, U. S. A. (JGA, QC)

Instituto de Ingenieria, Universidad Nacional Autonoma de Mexico,
Ciudad Universitaria, Coyoacan 04510, Mexico, D. F., Mexico (RQ, DA, RV, JMV, CP, GC)

## ABSTRACT

Accelerograms recorded on the Guerrero, Mexico, strong motion accelerograph network illustrate the dependence of strong ground motion on the magnitude and the hypocenter distance. These data support the hypothesis that complexity in accelerograms at short distances arises from complexity at the source. The duration of strong shaking is controlled by the source dimension at short distances, and extended by wave propagation effects as distance increases. Peak amplitudes (peak acceleration, velocity) saturate at different magnitudes at different distances. This change in shape of attenuation curves as magnitude increases can be explained by the transition of Green's functions from simple, short pulses at short distances to longer duration wave trains at large distances. Spectral amplitudes demonstrate scaling relations in which low frequency amplitudes are proportional to seismic moment but high frequencies increase much less rapidly. The beginnings of large earthquakes look like small earthquakes, consistent with a cascade model for the growth of large events. The most recent large earthquake, on Sept. 14, 1995 ($M_W$=7.4) shows surprisingly weak peak accelerations.

## KEYWORDS

Earthquakes, Guerrero, Mexico, Seismic Gap, Strong Motion, Peak Acceleration, Duration, Spectrum

## INTRODUCTION

This meeting, the Eleventh World Conference on Earthquake Engineering, is being held in Acapulco, Mexico. Acapulco is near the edge of the Guerrero gap, one of the most dangerous seismic gaps in the world. Because of its high potential to generate a magnitude 8 earthquake, we have operated a strong motion accelerograph network in Guerrero for the past decade. The purpose of the network is to record strong motion, on rock, from a great subduction zone earthquake. Although the anticipated great earthquake has, fortunately, not yet occurred, the network has recorded an outstanding collection of strong motion accelerograms from smaller earthquakes in the gap, and has also recorded some large earthquakes from neighboring gaps. This paper describes the current understanding of the Guerrero gap, reviews the characteristics of the Guerrero network, and summarizes some of the results from small to large earthquakes as we await the inevitable earthquake (or earthquakes) that will fill the Guerrero gap.

## GUERRERO SEISMIC GAP

Aftershock zones of large earthquakes near Guerrero are shown in Figure 1. The Guerrero gap is between the 1979 and 1957 ruptures. The largest recent historical earthquakes there were on January 24, 1899 (MW=7.9) and December 16, 1911 (MW=7.6). The turn of the century activity also included earthquakes on April 15, 1907 (M=7.7) and March 26, 1908 (M=7.6), centered near Acapulco and five earthquakes in the region with magnitudes between 6.9 and 7.3. The 1957 earthquake reruptured at least the eastern part of the 1907 zone. Anderson et al (1994) estimated that a seismic moment of a gap filling earthquake could

reasonably be $0.8 - 1.4 \times 10^{28}$ dyne-cm, and that a total moment of $2.0 \times 10^{28}$ dyne-cm is needed to accomodate the plate tectonic strains that are believed to have accumulated in the entire Guerrero - Ometepec region. Thus, a Guerrero gap earthquake could attain moment magnitude between 7.9 and 8.2.

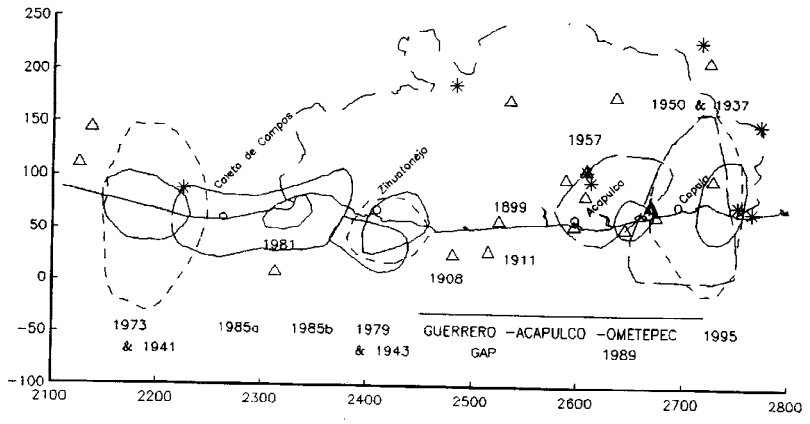


Figure 1. Approximate aftershock zones of large earthquakes along the coast of Guerrero since 1937 (modified from Anderson et al., 1994). Lighter dashed lines are earlier earthquakes. Triangles show epicenters of earthquakes with magnitudes 6.8 to 7.9 that occurred between 1899 and 1916. There were no major earthquakes in the region from 1917 through 1936. Approximate aftershock zone of the September 14, 1995 earthquake is from Anderson et al. (1995).

Nishenko and Singh (1987) estimated the conditional probability of a major earthquake in the Guerrero gap between 1986 and 1996 to be 56-79%. Since this window is nearly ended without the earthquake occuring, the probabilities for the next decade have increased. Notwithstanding formal probability estimates, it is important to keep in mind that every other part of the Mexican subduction zone from Jalisco to Oaxaca has ruptured since 1928. Considering the high overall rate of seismicity in Mexico, the Guerrero gap seems an extremely likely site for a large earthquake.

Two major earthquakes occurred in 1995 along the Mexican subduction zone. On September 14, an $M_W$=7.4 earthquake occurred near the eastern limit of Figure 1, as shown. Strong motion records from that earthquake will be discussed below. The second, on October 9 ($M_W$=7.9), occurred near the western boundary of the region covered by this map, and it is not shown. Thus, neither was in the Guerrero gap.

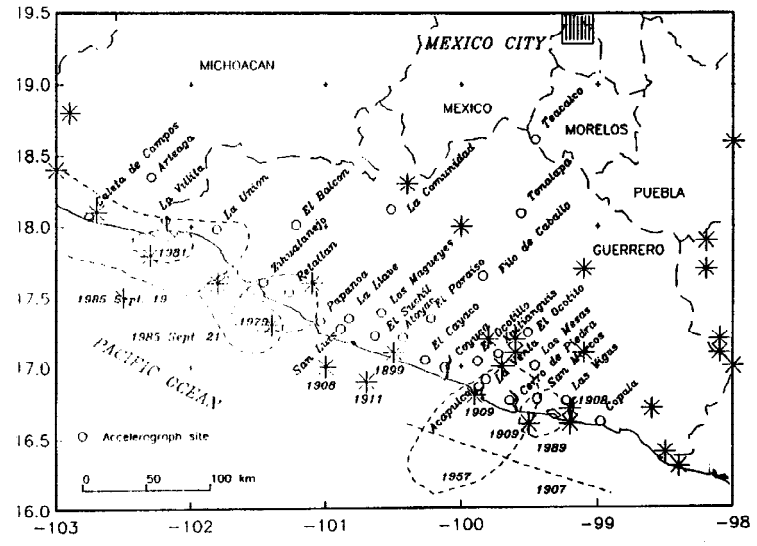


Figure 2. Map of Guerrero accelerograph network, in relationship to the aftershock zones of some of the major earthquakes shown in Figure 1.

Considering with its objectives, the 30 sites are on the best rock available, consistent with network geometry and secondary siting criteria. The instrumentation is described by Anderson et al (1994), and in more detail by Quaas et al. (1993b). Only digital instruments were considered from the very beginning, and the accessibility of small magnitude events and pre-event memory has thoroughly justified that decision, exceeding our expectations for both quality and quantity of data.

## GUERRERO ACCELEROGRAPH NETWORK

The Guerrero network (Figure 2) consists of 30 digital strong motion accelerographs in Guerrero, and neighboring states, Mexico. The network is described by Anderson et al (1994), and in more detail by Anderson and Quaas (1994). The primary objective is to record accelerograms from the anticipated large earthquakes, and a secondary objective is to record strong shaking from the smaller events to study scaling relations and attenuation, and their control by the source, and for use as empirical Green's functions.

Since 1985, on average the network has recorded about 130 accelerograms from about 55 earthquakes per year. The most important records have come from the Sept 19 and Sept 21, 1985 ($M_S$ = 8.1, 7.6), April 25, 1989 ($M_S$ = 6.9), and September 14, 1995 ($M_S$ = 7.4) earthquakes. At smaller magnitudes, the network has produced excellent sets of seismograms (about 10 or more records) from over 30 earthquakes with magnitudes 4.2 and up. Numerous smaller events, with magnitudes down to 3.0 and below, trigger only one

or a few stations. Humphrey and Anderson (1994) point out that locations are concentrated near the two ends of the Guerrero gap (Fig. 1). Records are documented in a series of annual reports and, for the most important events, in a short report for rapid examination and distribution of accelerograms. Anderson et al (1994) present a more thorough data summary.

We are currently rennovating the network with support of CONACYT and NSF. On all DCA-333 instruments, we are partially replacing the internal electronics and magnetic tape units with solid state memory devides but continuing to use the sensors and the cases, which are among the most expensive components of the system. For the DSA-1 accelerograph a similar prototype has been finished and is currently under test. These microcontroller-based upgrades also provide a better trigger device and a significantly longer pre-event memory, selectable up to 50 seconds, which will allow complete recordings of P-waves in more cases. In addition to these enhancements of older instruments we are replacing several units, especially those located around the Guerrero gap, with new state-of-the-art K2 accelerographs from Kinemetrics which are 19 bit digitizers and include GPS clocks. In January, 1996, 10 units had been received. All these changes and instrumental improvements, together with a technically skilled and motivated team of people in charge of the system, places this array as one of the best networks currently in Mexico and raises expectations of more and better quality data in the short future.

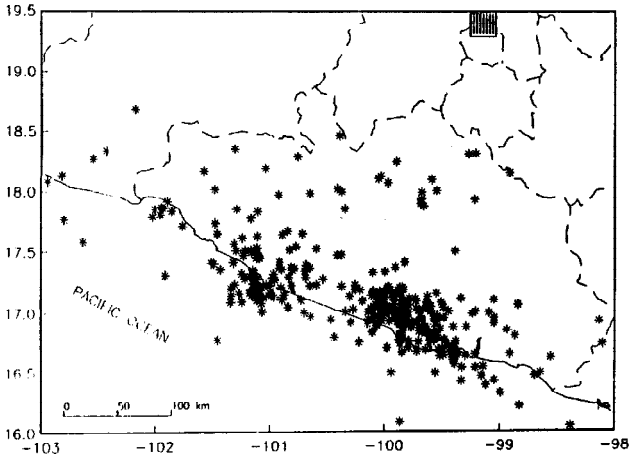


Figure 3. Epicenters of earthquakes recorded by the Guerrero network (Anderson et al, 1994).

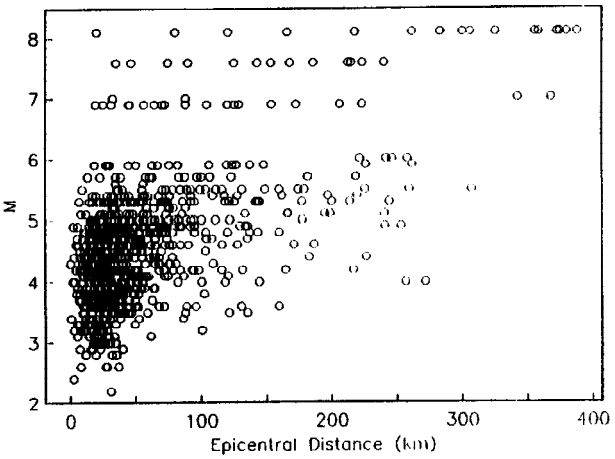


Figure 4. Magnitude and epicentral distance of earthquakes in Figure 3.

Figure 3 (from Anderson et al, 1994) shows the locations of 352 events recorded by the Guerrero accelerographs. These cluster at either end of the Guerrero seismic gap. Thus the Guerrero gap also appears to be a gap in the sense of having a depleted number of moderate sized (M4-6) earthquakes compared to adjacent regions. Figure 4 shows the magnitudes and distances of the events in Figure 3. There is a substantial number of records from short distances, for a large range of magnitudes from under 3.0 to 8.1.

## "SIMPLEST POSSIBLE ACCELEROGRAMS"

The Guerrero network has recorded several of what we term the "simplest possible accelerograms". From Aki and Richards (1980), in a homogeneous medium the far field displacement pulse including the P and S waves, $\mathbf{u}^F(\mathbf{x},t)$, is:

$$\mathbf{u}^{FP}(\mathbf{x},t) = \frac{\mathbf{A}^{FP}}{4\pi\rho\alpha^3 r}\dot{M}_0(t - r/\alpha) + \frac{\mathbf{A}^{FS}}{4\pi\rho\beta^3 r}\dot{M}_0(t - r/\beta) \qquad (1)$$

In Eq. (1), the source is located at the origin, $\mathbf{x}$ is the station location, $r$ is the source-station distance, $\rho$ is density, $\alpha$ and $\beta$ are P and S velocities, $\mathbf{A}^{FP}$ and $\mathbf{A}^{FS}$ are radiation patterns, $t$ is time, and $\dot{M}_0(t)$ gives the time derivative of the cumulative moment released as rupture progresses. Thus, both the far-field P and S waves have the form $u \sim \dot{M}_0(t)$. Figure 5 investigates the consequences of this relationship. The top time series shows a smooth functional form for $u \sim \dot{M}_0(t)$. It is not possible to have a simpler form than one that rises smoothly and monatonically from zero to the final seismic moment. Other time series in the figure show the time dependence of far field displacements, velocities, and accelerations that result, neglecting of course terms that affect the amplitude and sign. Thus, the acceleration trace in Figure 5 is the simplest form expected from a dislocation earthquake.

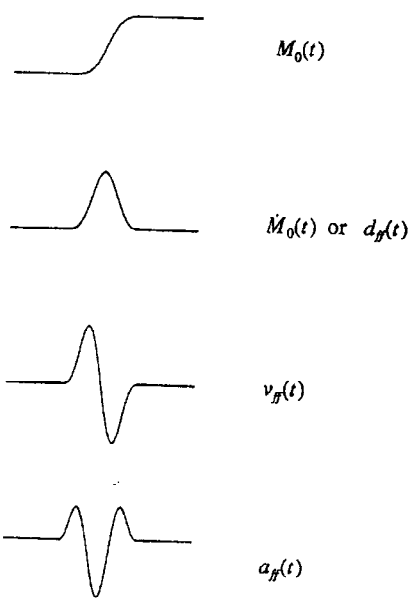


Figure 5. Illustration of a smooth source moment rate function, and consequent waveforms for far field displacement, velocity, and acceleration pulses in a homogeneous medium.

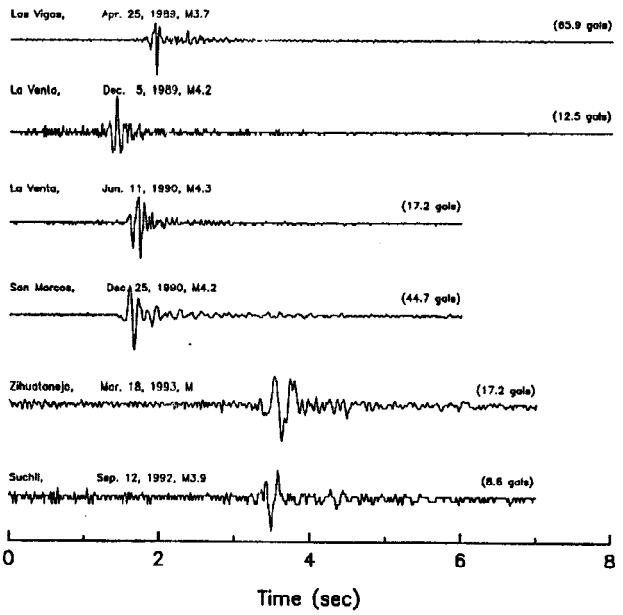


Figure 6. Several examples of accelerograms in which the S waveform resembles the simple form illustrated in Figure 5.

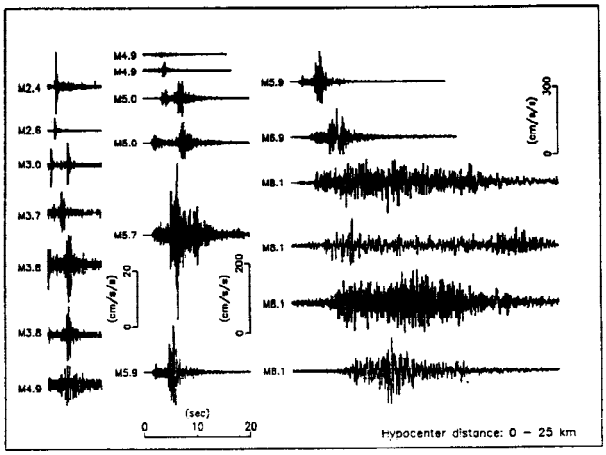


Figure 7. Selected accelerograms with hypocentral distance near 25 km. Amplitude scale changes between columns. The M4.9 event at bottom left is repeated at top center, and the M5.9 event at bottom center is repeated at top right.

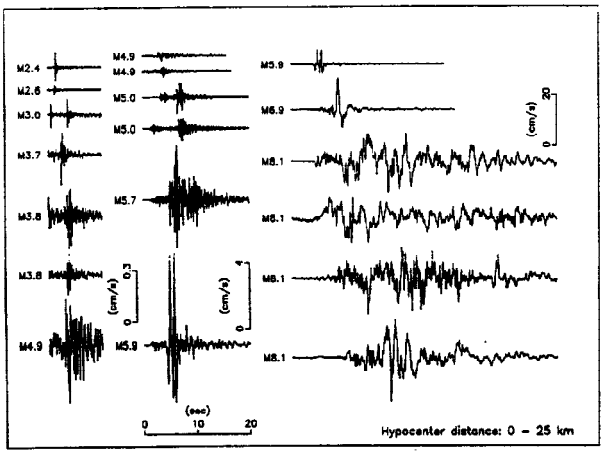


Figure 8. Velocities corresponding to Fig. 7. Although the peak accelerations do not increase significantly above M5.7, peak velocities for the M6.9 event are more than twice as large as for the M5.7 and 5.9 events, and a little smaller than for the M8.1 event.

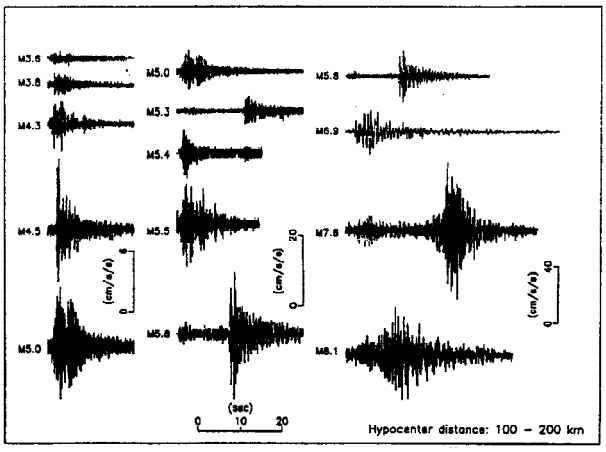


Fig. 9. Accelerograms for events at about 150 km.

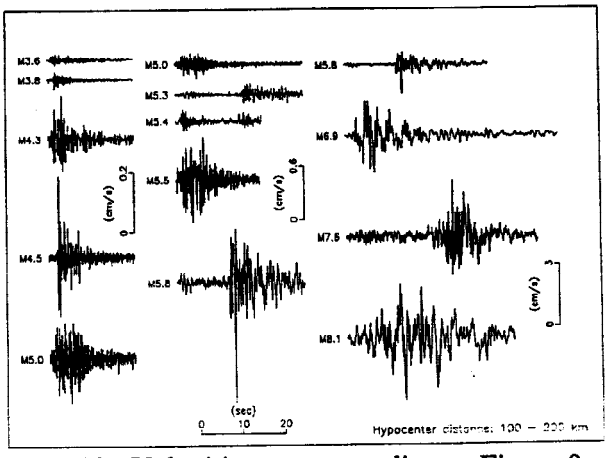


Figure 10. Velocities corresponding to Figure 9.

Figure 6 shows several accelerograms with nearly the simplest possible form. These are all from relatively small earthquakes. Anderson and Chen (1996) show several additional examples in which a nearby, larger earthquake is more complex, suggesting that the complexity comes from the source rather than from wave propagation effects. For the smaller earthquakes, attenuation might hide complexity at higher frequencies. At more distant stations, seismograms of the simple earthquakes in Figure 6 have waveforms with little resemblence to the simplest possible accelerograms in Figure 5, showing that wave propagation adds much complexity as distance increases. However, these examples suggest that site effects have been minimized.

## SCALING OF GROUND MOTIONS IN THE TIME DOMAIN

Chen (1996) developed examples of the changes in accelerograms with magnitude and hypocentral distance. Figures 7 to 10 show selected accelerations and velocities for earthquakes with magnitudes 2.4 to 8.1 and at distances of about 25 km and 150 km, to illustrate how these change with magnitude.

At short distances (Fig. 7) the peak accelerations in the M=5.7 earthquake are as large as for any of the larger events. This illustrates that acceleration saturates at about this magnitude at these distances, as seen previously (Anderson and Lei, 1994; Singh et al, 1988). On Fig. 8, the velocity from the M=6.9 earthquake equals that from the M=8.1 earthquake, suggesting that velocity saturation is taking place by about magnitude 7. Figs. 9 and 10, at the larger distance, differ, showing accelerations and velocities for earthquakes as large as 6.9 that are distinctly smaller than for the two largest events.

On Figures 7-10, the duration increases with the size of the earthquake. As noted previously (e.g. Hanks, 1979), the size of the fault controls both magnitude and duration. For example, Wells and Coppersmith (1994) found by regression that $M_W = 4 + \log A$, where A is the area of the fault in $km^2$. Most of the ruptures in this set (the M=8.1 event is the notable exception) can reasonably be assumed to be nearly circular. Thus the time for these faults to rupture (T) should generally be between T=r/v and T=2r/v, where r is the radius of a circle with area A. For v between 2 and 3 km/sec, these considerations imply that approximately, $M = 5.0 \pm 0.5 + 2 \log T$. Anderson and Chen (1996) show that this relationship forms an approximate lower bound to duration of the direct S waves.

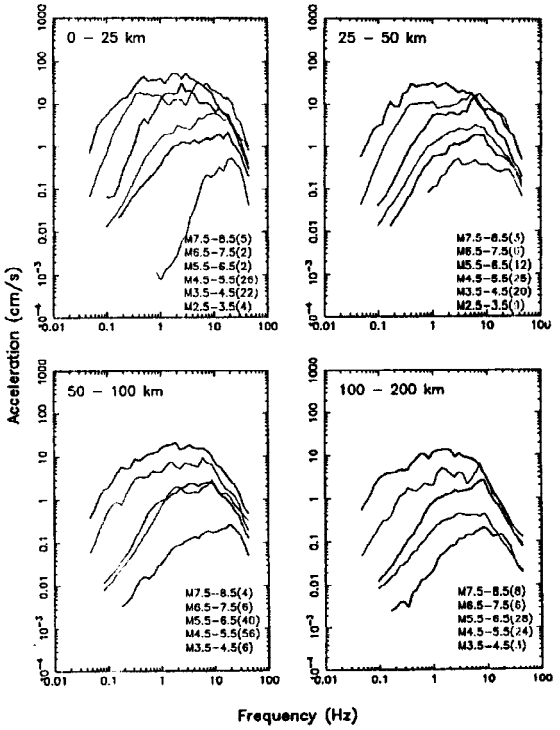


Figure 11. Averages of Fourier spectra from events in magnitude and distance bins, plotted to compare effect of magnitude at a fixed distance.

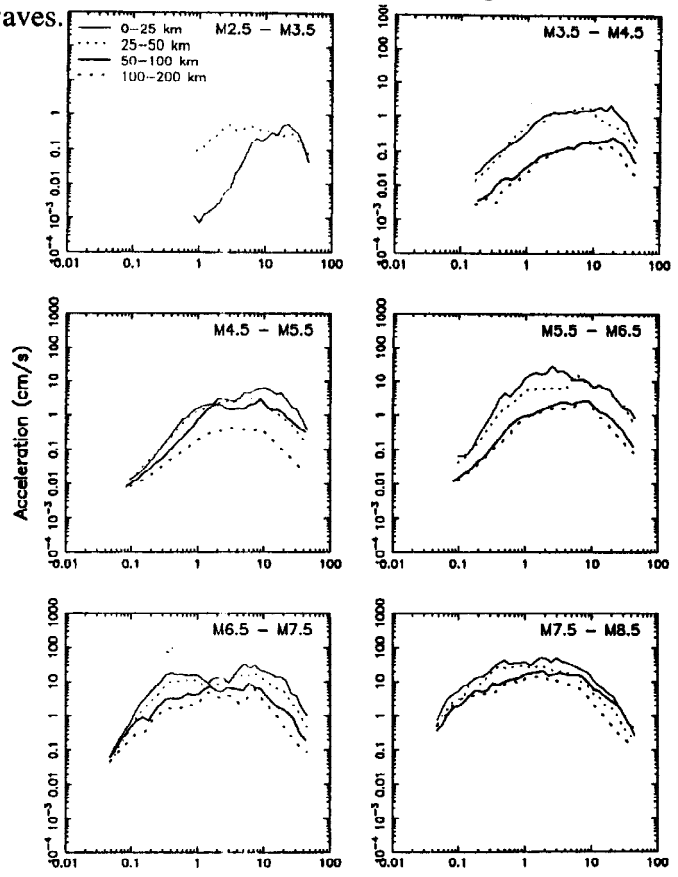


Figure 12. Averages of Fourier spectra from suites of events in magnitude and distance bins, plotted to compare effect of distance at a fixed magnitude.

## SCALING IN THE FREQUENCY DOMAIN

Figures 11 and 12, from Anderson and Chen (1996), show average Fourier amplitude spectra as a function of magnitude and distance, respectively. In Fig. 11 there is a major change in spectral shapes as magnitude increases, with a much more rapid growth of low frequency energy than high frequency energy as magnitude increases. Irregularity between magnitude groups is caused by the uneven distibution in magnitudes of events forming the average. At high frequencies, there is an apparent increase in $f_{max}$ (Hanks, 1984) from about 10 Hz for M=8 to about 20 Hz for M=3. This could be from the interaction of the corner frequency with spectral shape (e.g. Anderson, 1986). With distance, there is less than a factor of 10 difference in amplitude, and little change in spectral shape between the 0-25 km group and the 100-200 km group (Figure 12), consistent with results by Humphrey and Anderson (1992).

## SATURATION

As noted above, the peak values of acceleration and velocity seem to saturate at a larger magnitude at large distances than at small distances. This cannot be attributed to a difference in frequency content (Fig. 12). We propose instead that it is the result of multi-path arrivals resulting in multiple parts of the fault contributing at the same time. At short distances, the Green's functions are relatively simple (Fig. 6), while at large distances they last longer (e.g. compare Figure 7 with Figure 9). Thus, at short distances a smaller small part of the fault is contributing to the total wavefield at any one time. The saturation magnitude results from an interaction of the duration of the faulting process and the duration of the Green's function. Saturation occurs at the magnitude where the duration of the fault rupture process exceeds the duration of significant arrivals in the Green's function.

## BEGINNINGS OF EARTHQUAKES

Anderson and Chen (1995) studied the beginnings of earthquakes on the first 3.5 seconds of P-wave accelerograms. The problem has a practical application for seismic alerts like here in Mexico (Espinosa et al., 1995), and earthquake physics. Figure 13 is representative of results from Anderson and Chen (1995).

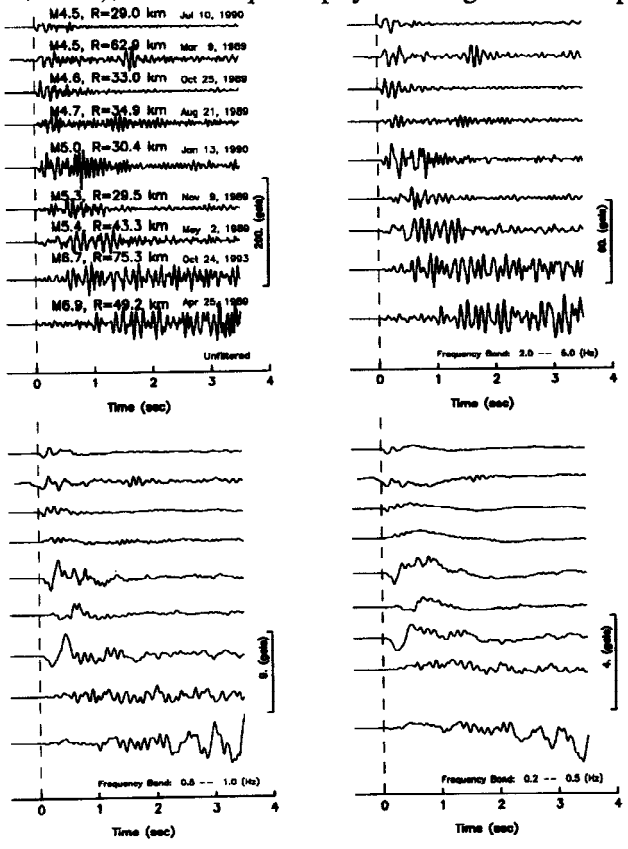


Figure 13. Initial 3.5 sec. of P-wave accelerograms (vertical) from Las Mesas. Amplitudes are normalized to 25 km. Original (upper left) and causal filtered (pass band indicated) records are on a common amplitude scale within each portion of the plot. Note that differences between small and large earthquakes tend not to appear during the first second of motion. (from Anderson and Chen, 1996).

During the initial 0.5 seconds, the unfiltered records show no significant difference between smallest and largest events. Filtered in the 2-5 Hz band the smallest events begin more sharply than the largest events. At lower frequencies, seismograms of the largest events show a complex series of multiple pulses, but there is no convincing tendency for the large asperities to appear early in the records.

Prolonged duration is a more reliable indication that a significant earthquake is underway. For events with magnitudes less than about 5.5, P-wave amplitudes are decreasing after about 2 seconds. Vertical P-wave amplitudes that are sustained or increasing through the first 3.5 seconds (until the arrival of the S-wave) characterize larger earthquakes.

Anderson and Chen (1995) concluded that these observations are consistent with a cascade-like model of faulting in which the largest asperities are located at random on the eventual fault plane, and fail when the rupture front, propagating from the hypocenter, reaches them. Occasionally, the largest asperities may be at the hypocenter and thus fail immediately, but for a large fault they are more likely to be located elsewhere and to fail later. We are eager to see if the new 16 bit accelerographs will detect significant differences in the initial P-waves at lower frequencies.

# COPALA EARTHQUAKE, SEPTEMBER 14, 1995 ($M_W$=7.4)

Anderson et al (1995) gave a preliminary report on the Copala, Guerrero, Mexico earthquake. It occurred just beyond the eastern limit of the Guerrero network (Fig. 2), and triggered the two stations within 50 km of the epicenter, and an estimated 300 to 400 stations in total. It also triggered the seismic alert system, which successfully issued a warning in Mexico City before strong shaking arrived.

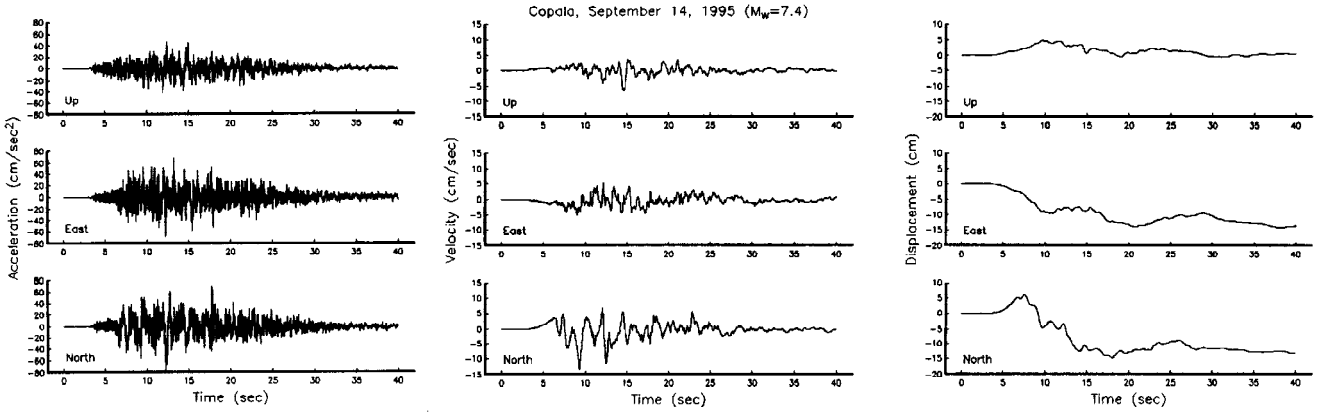


Figure 14. Acceleration, and corresponding inferred velocity and displacement, from the Copala accelerogram for the September 14 earthquake ($M_W$=7.4). The Copala station is at a hypocentral distance of 24 km, based on S-P time. The epicenter is 10-15 km southeast of the station, and the dominant direction of rupture propagation is away from the station towards the east.

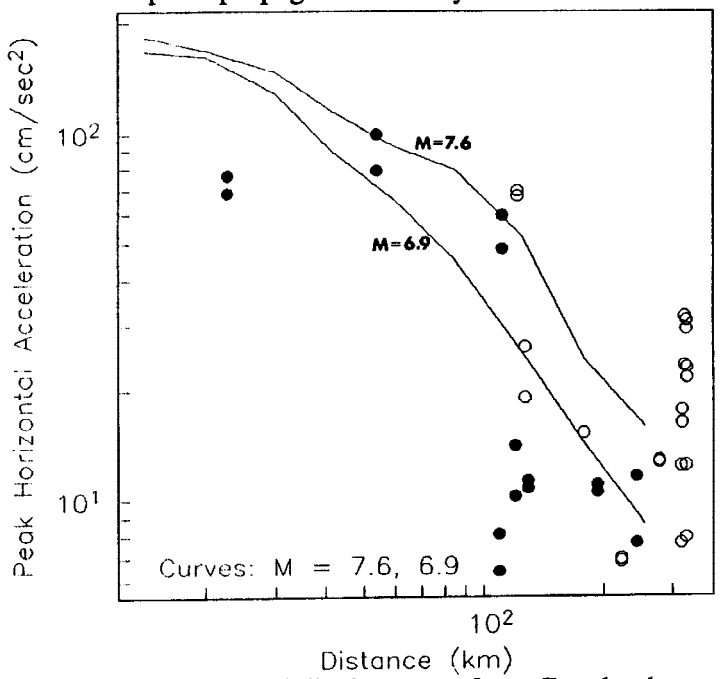


Figure 15. Peak accelerations from rock (solid symbols) and soil (open symbols) stations from the Copala earthquake. Curves give peak accelerations from the nonparametric regression of Anderson and Lei (1994) for this region. After Anderson et al (1995).

Acceleration, velocity, and displacement from Copala, the nearest station, is shown in Figure 14 (from Anderson et al 1995). Figure 15 shows peak accelerations from this earthquake at several of the stations in and outside of the Guerrero network. The surprising feature of this earthquake is the low values of peak acceleration, even compared to past experience in Guerrero, as shown by the nonparametric attenuation curves (Anderson and Lei, 1994) for magnitudes 6.9 and 7.6. Points for rock sites are mostly about a factor of two smaller than what is expected for a magnitude 6.9 earthquake. Peak velocities (Fig. 14) at the nearest station are under 15 cm/sec, and thus are similar to those in previous events (Fig. 8), and like those show a complex sequence of pulses. Displacements have the same nature as those seen at Caleta de Campos in the 1985 Michoacan earthquake (Anderson et al., 1986). Integration of the north-south component in particular, according to Anderson et al (1995), suggests a static offset with a rise time of about 10 seconds, much like the Caleta de Campos record. The direction and amplitudes of the static offsets inferred here are plausible based on a simple dislocation model for the earthquake. The similar velocities and displacements to Caleta de Campos in 1985 suggest that the 1995 earthquake was the result of the failure of a single, complex

asperity similar to the asperity near Caleta de Campos. The difference between 1985 and this earthquake is that in 1985 the rupture continued on for a much greater distance, and broke another major asperity centered perhaps 80 km away from the hypocenter, while this earthquake did not continue in that manner. If the hypocenter had, by chance, been at the eastern edge of the rupture instead of the western edge, it is possible that the event could have continued farther towards the Guerrero gap.

## ACKNOWLEDGEMENTS

This research has been supported by the U. S. National Science Foundation under a series of grants, most recently grants BCS 9120027 and CMS 9506675, and by the Instituto de Ingenieria at the Universidad Nacional Autonoma de Mexico.

## REFERENCES

Aki, K. (1967). Scaling law of seismic spectrum, J. Geophys. Res. 72, 1217-1231.

Aki, K. and P. G. Richards (1980). Quantitative Seismology Theory and Methods, Vol. I, W. H. Freeman and Company, New York, 557 pages.

Anderson J. G. and Q. Chen (1995a). Beginnings of Earthquakes in the Mexican subduction zone on strong-motion accelerograms, Bull. Seism. Soc. Am., 85, 1107-1115.

Anderson J. G. and Q. Chen (1995b). Illustrations of dependence of strong ground motions on magnitudes and hypocenter distances, (in preparation).

Anderson J. G. and Y. Lei (1994). Nonparametric description of peak acceleration as a function of magnitude, distance, and site in Guerrero, Mexico, Bull. Seism. Soc. Am., 84, 1003-1017.

Anderson, J. G. and R. Quaas, editors (1994a). *Guerrero, Mexico, Accelerograph Network: Network Description*, Report GAA 15, Seismological Laboratory, University of Nevada, Reno, 90 pages.

Anderson, J. G., P. Bodin, J. Brune, J. Prince, S. Singh, R. Quaas, M. Onate, and E. Mena (1986). Strong ground motion and source mechanism of the Mexico earthquake of September 19, 1985, Science 233, 1043-1049.

Anderson, J. G., S. K. Singh, J. M. Espindola and J. Yamamoto (1989a). Seismic strain release in the Mexican subduction thrust, Physics of the Earth and Planetary Interiors 58, 307-322.

Anderson, J. G., S. K. Singh, J. M. Espindola and J. Yamamoto (1989b). Seismic strain release in the Mexican subduction thrust, Physics of the Earth and Planetary Interiors, 58, 307-322.

Anderson, J. G., J. Brune, J. Prince, Roberto Quaas, S. K. Singh, David Almora, Paul Bodin, Mario Onate, Ricardo Vasquez, and Juan Manuel Velasco (1994). The Guerrero Accelerograph Network, Geofisica Internacional, Vol. 33, pp. 341-371.

Anderson, J., R. Quaas, S. K. Singh, J. M. Espinosa, A. Jimenez, J. Lermo, J. Cuenca, F. Sanchez-Sesma, R. Meli, M. Ordaz, S. Alcocer, B. Lopez, L. Alcantara, E. Mena, C. Javier (1995). The Copala, Guerrero, Mexico Earthquake of September 14, 1995 ($M_W$=7.4): A Preliminary Report, Seismological Research Letters 66, No. 6, 11-39.

Anderson J. G., J. N. Brune, J. Prince, R. Quaas, S. K. Singh, D. Almora, P. Bodin, M. Onate, R. Vasquez, and J. M. Velasco (1994a). The Guerrero accelerograph network, Geofisca Internacional, Vol. 33, pp. 341-371. Mexico city, Mexico.

Chen, Q. (1996). M.S. Thesis, University of Nevada, Reno (in preparation).

Espinosa-Aranda, J. M., A. Jimenez, G. Ibarrola, F. Alcantar, A. Aguilar, M. Inostroza, and S. Maldonado (1995). Mexico City seismic alert system (this issue).

Hanks, T. C. (1979). b values and $\omega^{-\gamma}$ seismic source models: implications for tectonic stress variations along active crustal fault zones and the estimation of high-frequency strong ground motion, JGR 84, 2235-2242.

Hanks, T. C., $f_{max}$, Bull. Seismo. Soc. Am., 74, 1867-1880.

Humphrey, J. R. Jr., and J. G. Anderson, (1992). Shear-wave attenuation and site response in Guerrero, Mexico, Bull. Seismo. Soc. Am., 81, 1622-1645.

Humphrey, J. R. Jr., and J. G. Anderson, (1994). Seismic source parameters from the Guerrero subduction zone, Bull. Seismo. Soc. Am., 84, pp. 1754-1769.

Nishenko, S. P. and S. K. Singh (1987). Conditional probabilities for the recurrence of large and great intraplate earthquakes along the Mexican subduction zone, Bull Seism. Soc. Am. 77, 2095-2114.

Quaas, R., J. G. Anderson, D. Almora, J. M. Velasco, R. Vazquez (1993b). Guerrero Accelerograph Network: Instrumentation, in J. G. Anderson and R. Quaas, editors, *Guerrero, Mexico, Accelerograph Network: Network Description*, Report GAA-15, Seismological Laboratory, University of Nevada, Reno.

Singh, S. K., M. Ordaz, J. G. Anderson, M. Rodriguez, R. Quaas, E. Mena, M. Ottaviani and D. Almora (1989a). Analysis of near-source strong motion recordings along the Mexican subduction zone, Bulletin of the Seismological Society of America 79, 1697-1717.

Wells D. L., and K. J. Coppersmith (1994). New empirical relationships among magnitude, rupture length, rupture width, rupture area and surface displacement, 84, 974-1002.

Yu, G. (1994). Some aspects of earthquake seismology: slip partitioning along major convergent plate boundaries; composite source model for estimation of strong motion; and nonlinear soil response modeling, Ph.D. Thesis, University of Nevada, Reno, 144 pages.

Zeng Y., Yu, G., and J. G. Anderson (1994). A composite source model for computing realistic synthetic strong ground motions, Geophys. Res. Lett., 21, 725-728.